Reznychenko, M., Bogomaz, O., Kotov, D., Zhivolup, T., Martynova, K., Burmaka, V., & Kolodyazhnyi, V. (2026). Ionospheric response to the weak geomagnetic storm of 1—2 February 2025 in the Weddell Sea Anomaly region: observations from Ukrainian Antarctic Akademik Vernadsky station. *Ukrainian Antarctic Journal*, *24*(1), 50—59.
https://doi.org/10.33275/1727-7485.1.2026.757

Ionospheric response to the weak geomagnetic storm of 1—2 February 2025 in the Weddell Sea Anomaly region: observations from Ukrainian Antarctic Akademik Vernadsky station

Maryna Reznychenko [1, 2, *], Oleksandr Bogomaz [1, 3], Dmytro Kotov [1], Taras Zhivolup [1], Kateryna Martynova [1], Viktor Burmaka [1], Vyacheslav Kolodyazhnyi [1]

[1] Institute of Ionosphere, National Technical University "Kharkiv Polytechnic Institute", Kharkiv, 61002, Ukraine
[2] Space Research Centre of Polish Academy of Sciences, Warsaw, 00-716, Poland
[3] Institute of Radio Astronomy, National Academy of Sciences of Ukraine, Kharkiv, 61002, Ukraine

* **Corresponding author:** mrezn.cbk@gmail.com

Abstract. The ionospheric response to the weak geomagnetic storm of 1—2 February 2025 was studied within the Weddell Sea Anomaly region. The behavior of the key ionospheric parameters (N_mF_2 and h_mF_2) was analysed using ionosonde observations from the Ukrainian Antarctic Akademik Vernadsky station and vertical total electron content derived from Global Navigation Satellite System measurements. A pronounced nighttime depletion was observed in both ionosonde F2-layer peak electron density (N_mF_2) and the total electron content values on 1 and 2 February 2025. This indicates the development of the negative phase of the ionospheric storm and a weakening of the Weddell Sea Anomaly under minor geomagnetic disturbances. N_mF_2 decreased by a factor of ~2 on 1 February and by a factor of ~5 on 2 February, while the total electron content was reduced by ~15—20 TECU and ~25 TECU, respectively. The negative phase penetrated farther toward the equator on 1 February, whereas on 2 February it remained restricted to high- and mid-latitude regions. Notably, such a strong depletion in N_mF_2 occurred despite a significant uplift of the F2-layer peak height (h_mF_2) by ~60—70 km. No clear signatures of vertical plasma transport driven by the penetration electric field of magnetospheric origin were found in the observed h_mF_2 variations. The likely reason for such a depletion in ionospheric plasma density is storm-time changes in neutral composition associated with upwelling, reduction in the O/N_2 ratio, and transport of the composition disturbance zone by thermospheric winds from high to low latitudes. These results demonstrate that even minor geomagnetic storms can substantially modify the ionosphere—thermosphere system over Antarctica and significantly impact the Weddell Sea Anomaly.

Keywords: electron density, F2-layer, ionosonde, ionosphere, ionospheric storm, negative phase

1 Introduction

Geomagnetic storms and substorms, driven by increased solar wind energy input into the magnetosphere associated with coronal mass ejections and/or high-speed solar wind streams, produce disturbances in the Earth's ionosphere known as ionospheric storms. Depending on the balance between storm-time electrodynamic forcing, neutral winds, and thermospheric composition changes, ionospheric storms can lead to enhancement or depletion of the F2-layer peak electron density (N_mF_2) and total electron content (TEC). These ionospheric responses are commonly referred to as positive or negative ionospheric storm phases, respectively (Gonzalez et al., 1994; Buonsanto, 1999; Prölss, 2004; Mendillo, 2006). In many cases, storm-time perturbations are accompanied by significant changes in the F2-layer peak height (h_mF_2), reflecting vertical plasma transport driven by storm-induced neutral winds and/or electric fields (Prölss, 1997). The ionospheric responses depend on such factors as storm onset time, season, local time, geographic and geomagnetic location (latitude and longitude), and solar cycle conditions (Fuller-Rowell et al., 1996; Gao et al., 2008; Fuller-Rowell, 2011; Borries et al., 2015).

High-latitude regions play a key role in driving ionospheric storm dynamics. Enhanced Joule heating and particle precipitation in the auroral zones lead to thermospheric heating and expansion, increasing the neutral density at the higher altitudes and driving the upward transport ("upwelling") of heavier molecular species (N_2 and O_2) from below, as well as to horizontal redistribution of disturbed neutral composition toward the lower latitudes. This process reduces the atomic oxygen (O) density and increases the recombination rate, particularly by converting O^+ to molecular ions (O_2^+, NO^+), which then rapidly recombine with electrons. As a result, the F2-layer peak electron density decreases, producing a negative ionospheric storm (Fuller-Rowell et al., 1994; Buonsanto, 1999; Prölss, 2004).

The Antarctic ionosphere is particularly sensitive to high-latitude forcing due to its proximity to the auroral oval. During the Antarctic summer, the thermosphere is characterised by increased exospheric temperatures and scale heights, and by pronounced seasonal changes in neutral composition associated with summer-to-winter circulation (Fuller-Rowell et al., 1994; Qian et al., 2009; Emmert, 2015). Storm-time energy input can further enhance neutral wind circulation and composition disturbances, which in turn affect both the vertical ionospheric structure and plasma density variations. A prominent feature of the Antarctic ionosphere is the Weddell Sea Anomaly (WSA), a persistent summer phenomenon characterised by enhanced nighttime electron density compared to daytime values. The WSA is generally caused by the combined effects of photoionisation, thermospheric winds, and associated wind-driven field-aligned plasma transport. It is also highly sensitive to changes in neutral dynamics and composition (Bellchambers & Piggott, 1958; Dudeney & Piggott, 1978; Horvath & Essex, 2003). Geomagnetic disturbances can therefore modify or disrupt the typical WSA pattern by affecting thermospheric circulation and composition.

Despite numerous studies of ionospheric storms, many investigations have predominantly focused on strong geomagnetic events and on the Northern Hemisphere (Correia et al., 2017; Mansilla, 2017; de Abreu et al., 2023; Melendi et al., 2025; Chakraborty & Seemala, 2026), while the effects of weak to moderate disturbances, particularly over Antarctica, remain less explored. Chen et al. (2022) suggested that frequent weak geomagnetic activities modulate the ionosphere from high to low latitudes primarily through disturbances in high-latitude thermospheric composition, associated with polar thermospheric upwelling and altered background thermospheric circulation.

In this study, we investigate the ionospheric response over Antarctica to a weak geomagnetic storm that occurred during February 1–2, 2025. The analysis is based on ionosonde measurements at the Ukrainian Antarctic Akademik Vernadsky station (hereinafter – Vernadsky Station) (geographic coordinates: 65.25°S 295.75°E; geomagnetic coordinates: 55.8°S 6.3°E) and GNSS-based products. We examine storm-time variations in the F2-layer peak electron density and height, as well as vertical total electron content (VTEC). These results provide new insight into the WSA response to minor geomagnetic disturbances over Antarctica.

2 Data and methods

The data used in the paper were obtained by two software-defined radio (SDR)-based ionosondes operating at Vernadsky Station (Koloskov et al., 2023). Ionograms were obtained every 15 minutes. The ionosonde operated in the 1–16 MHz frequency range with 320 discrete frequencies, covering a virtual height range of 92–655 km with 750 sampling points, and using a transmitter pulse width of 600 μs (16 sub-pulses of 37.5 μs).

Ionograms were manually scaled using the IonogramViewer2 program version 1.7.1 (https://github.com/Albom/IonogramViewer2/releases/download/v.1.7.1/IonogramViewer2-1.7.1.zip). The obtained critical frequencies of F2, F1, and E layers and traces were used for electron density profile inversion using the NHPC program version 4.30 (Huang & Reinisch, 1996) and further calculation of the F2-layer peak height. The F2-layer peak electron density N_mF_2 was calculated from the critical frequency of the F2-layer f_oF_2 using the relation (Piggott & Rawer, 1972):

$$N_mF_2 = 1.24 \cdot 10^{10} \cdot f_oF_2^{\,2}, \quad (1)$$

where f_oF_2 is expressed in MHz.

The vertical TEC data were provided from Global Positioning System (GPS) measurements by UPC-IonSAT with a tomographic-kriging technique (UQRG GIM) (Hernández-Pajares et al., 2009; 2011; 2017). The VTEC is measured in TEC units (TECU), with 1 TECU equal to 10^{16} electrons · m^{-2}.

To determine the solar-wind energy input into Earth's magnetosphere, the Akasofu ε function was calculated according to formula (Perreault & Akasofu, 1978; Akasofu, 1981):

$$\varepsilon = \frac{V_{sw} \cdot B^2_{total} \cdot \sin^4(\theta/2) \cdot l_0^2}{\mu_0}, \quad (2)$$

where V_{sw} is the solar wind speed (km · s^{-1}), and B_{total} is the magnitude of the interplanetary magnetic field (IMF). The parameter θ is the IMF clock angle, $\theta = \arctan(B_y/B_z)$, with B_y and B_z in geocentric solar magnetospheric coordinates. The scale length l_0 is a length related to the radius of cross-section of the magnetosphere, estimated to be $l_0 = 7 \cdot R_e$, where $R_e = 6371$ km is Earth's radius. The constant $\mu_0 = 4\pi \cdot 10^{-7}$ H · m^{-1} is the permeability of free space.

3 Results and discussion

3.1 Solar and geomagnetic conditions

Figure 1 shows variations in solar, geomagnetic, and auroral activity indices and the Akasofu function from 30 January to 4 February 2025. The analysed interval coincides with local summer conditions in Antarctica. The solar activity during the investigated period was high (solar radio flux index $F_{10.7}$ ranged from 184 to 220 sfu). Geomagnetic activity was quiet from 30 to 31 January (K_p was mostly less than 2+ and did not exceed 3–) and from 3 to 4 February (K_p < 2–), while during 1 and 2 February 2025, an increase in geomagnetic activity was observed (K_{pmax} = 4+). According to the National Oceanic and Atmospheric Administration (NOAA) Geomagnetic Storm Scale, this was classified as a boundary between active conditions and a minor geomagnetic storm (G1), which begins at K_p = 5 (https://www.swpc.noaa.gov/noaa-scales-explanation).

It can be seen that a rapid increase in energy input (ε reaching ~80 GW) began around noon by UT on 31 January 2025, with a maximum of approximately 120 GW near 18:00 UT. This enhanced energy injection is consistent with a magnetopause compression and the associated sudden storm commencement (SSC), followed by the development of the storm's main phase at ~01:00 UT on 1 February 2025, during which SYM-H gradually decreased to about –30 nT. After the passage of the magnetic cloud, the ε value dropped significantly around midnight on 1 February and auroral activity began to increase. From 1 February to the end of 2 February, a series of AE ("auroral electrojet") index bursts were observed in auroral latitudes with values reaching $AE_{max} \approx 1200$ nT, indicating strong substorm activity. The interplanetary electric field component (E_y) fluctuated significantly from –6 to +6 mV · m^{-1}.

3.2 Results of ionosonde observations over the Vernadsky Station

Figure 2 shows diurnal variations of the key ionospheric parameters (f_oF_2, N_mF_2, and h_mF_2) obtained using the ionosonde located at Vernadsky Station during January 30 – February 4, 2025.

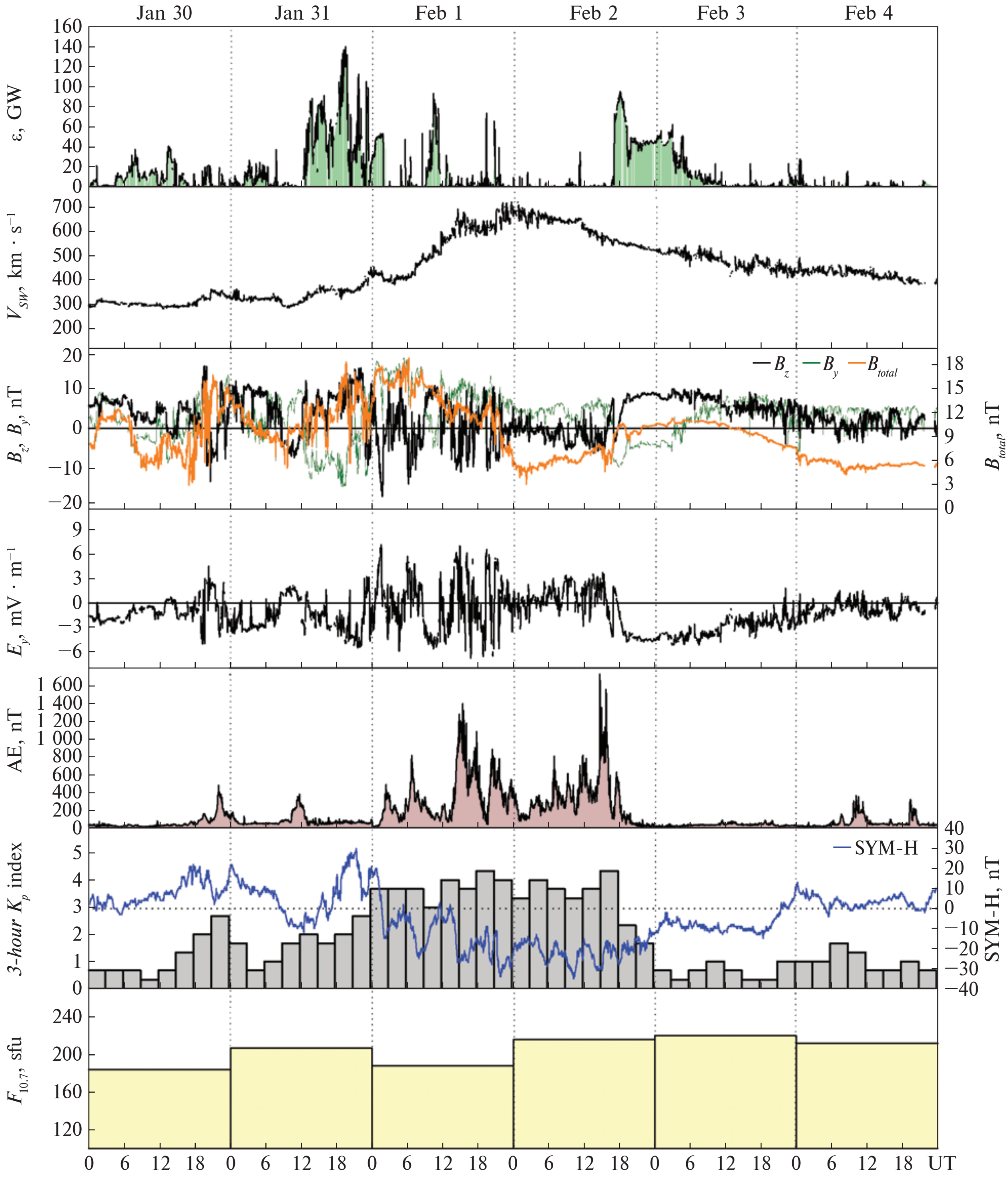

Figure 1. Variations of parameters describing space weather during 30 January – 4 February, 2025. From top to bottom, the panels show the Akasofu function (ε), the solar wind speed (V_{SW}), the total magnitude of the IMF (B_{total}) (orange line), the IMF Bz (black line) and By (green line) components, the interplanetary electric field component (E_y), the auroral electrojet index (AE), the 3-hour planetary K_p index (gray bars), the SYM-H index (blue line), and the daily solar radio flux ($F_{10.7}$). The time is in Coordinated Universal Time (UT)

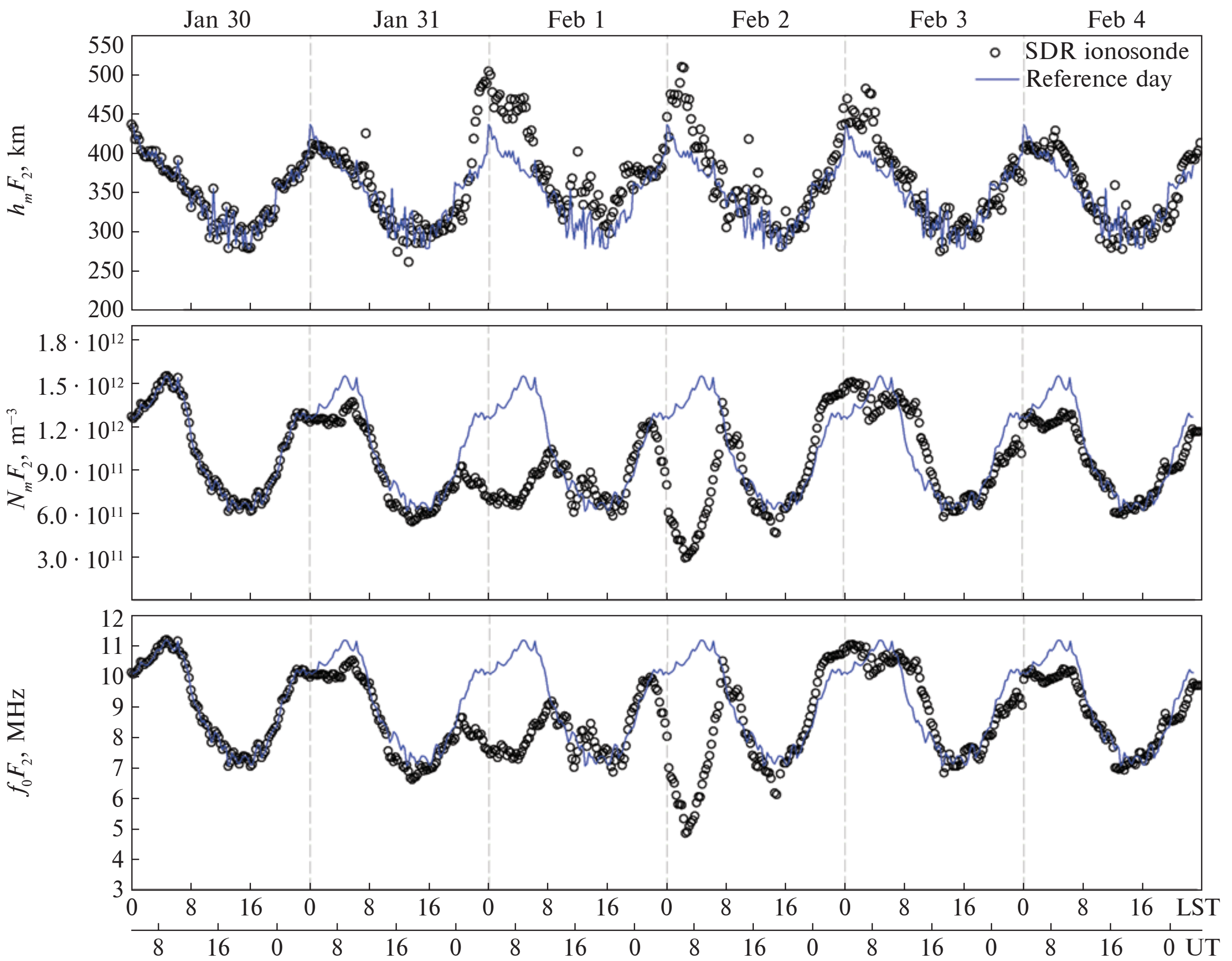

Figure 2. Diurnal variations of critical frequency (f_oF_2), F2-layer peak electron density (N_mF_2), and height (h_mF_2) over Vernadsky Station during 30 January – 4 February, 2025. The open circles show observations. The solid blue lines show the f_oF_2, N_mF_2, and h_mF_2 variations from the quiet reference day (30 January 2025), repeated for other days. The time is in UT and Local Solar Time (LST = UT – 4.28 h)

A prominent feature of the Antarctic ionosphere in summer is the WSA, which is clearly evident over Vernadsky Station during the investigated period. Under quiet geomagnetic conditions, both prior to the storm (30–31 January) and after it (3–4 February), the observed N_mF_2 at local midnight was about a factor of 2 higher than at local noon.

The onset of the main phase of the magnetic storm, around midnight by UT (~20:00 LT) on 31 January – 1 February, 2025, caused an interruption in the evening increase of N_mF_2 and a subsequent decrease to a value typical of the daytime quiet period (~6 · 10^{11} m^{-3}) on January 30. A clearly pronounced negative phase of the ionospheric storm was observed, manifested as a dip in the variations of f_oF_2 and N_mF_2, reaching a local minimum at ~04:00 LT. At the same time, h_mF_2 increased by ~60 km relative to the quiet reference day on 30 January 2025. During the daytime hours (11:00–14:00 LT) on 1 February, a moderate increase in N_mF_2 (by ~13%) was observed. At the same time, h_mF_2 increased by ~35 km, indicating a weak positive phase of the ionospheric storm.

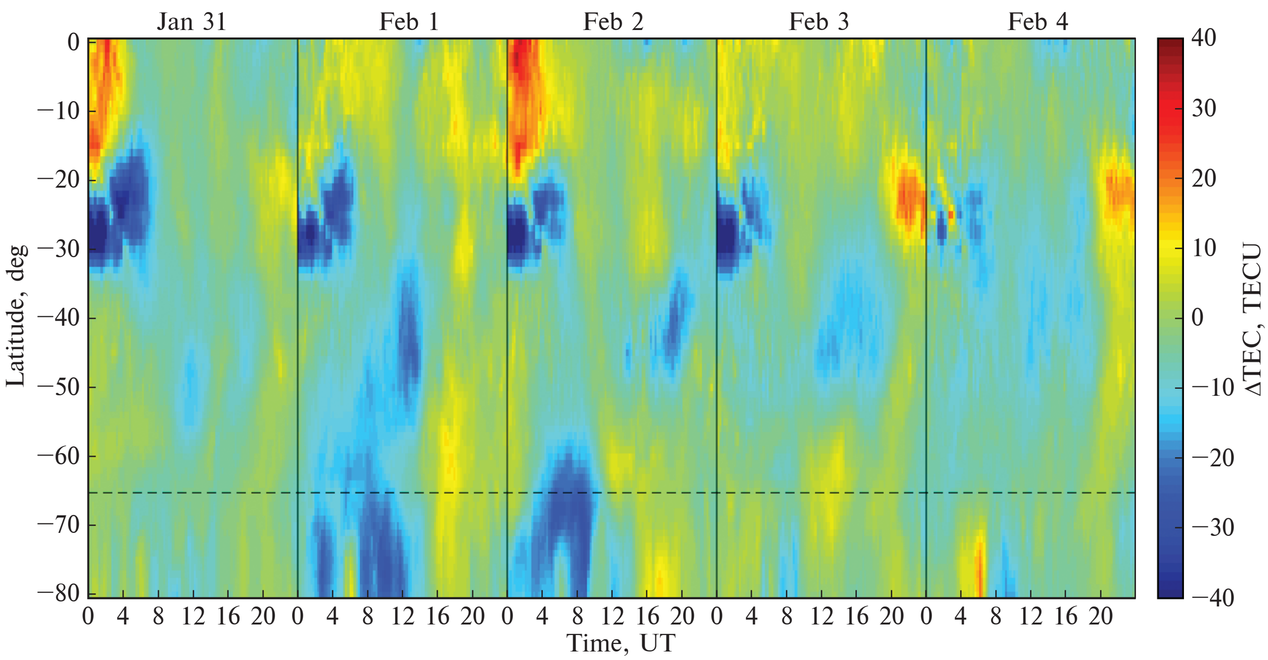

Figure 3. Latitude-time distribution of differential ΔTEC relative to the reference day (30 January 2025) at 295.75°E during 31 January — 4 February 2025. The dashed black line shows the latitude of Vernadsky Station (65.25°S)

During the night of 1—2 February 2025, a gradual decrease in N_mF_2 was observed beginning at ~22:00 LT on 1 February, reaching a local minimum at ~02:45 LT. Compared with the geomagnetically quiet day on 30 January 2025, N_mF_2 was approximately five times smaller. During this interval (around 22:00—02:45 LT), h_mF_2 increased by ~70 km. After this, the ionosphere began to return to its pre-storm conditions, and by ~08:00 LT on 2 February 2025, N_mF_2 reached the quiet-time values (~$1.2 \cdot 10^{12}$ m^{-3}). The nighttime uplift of the ionosphere by ~35 km on 2—3 February (00:00—04:00 LT) was accompanied by a slight decrease in N_mF_2 (by ~13%).

3.3 Results of TEC observations

Figure 3 shows the diurnal distribution of differential ΔTEC at 295.75°E in the Southern Hemisphere (80°S — 0°), derived by subtracting the TEC values on a geomagnetically quiet reference day (30 January 2025) from those obtained from 31 January to 4 February 2025. A pronounced depletion in VTEC is observed on 1 and 2 February at the latitude of the Vernadsky Station, representing a clear signature of the negative phase of the ionospheric storm. As can be seen, on 1 February, TEC values decreased by ~15—20 TECU from ~02:00 UT to 13:00 UT, while on 2 February the depletion reached ~25—30 TECU between ~04:00 — 10:00 UT. Notably, on 1 February the intensity of the negative phase expanded toward lower latitudes to ~30°S, whereas on 2 February it was mostly confined to high- to mid-latitudes, extending to ~55°S.

3.4 Discussion

Given that the austral summer occurs over Antarctica during the boreal winter months, the background thermospheric circulation is directed from the Southern Hemisphere toward the Northern Hemisphere. Additional heating associated with the substorm activity could further enhance this circulation by strengthening equatorward meridional neutral winds, thereby lifting the ionosphere along geomagnetic field lines during nighttime or significantly reducing its descent during daytime. The resulting upward motion of h_mF_2 during local nighttime to higher altitudes, where recombination rates are lower, allows the ionospheric plasma to persist longer. Such an uplift of the F2-layer is clearly evident over Vernadsky Station during the disturbed nights of 1 and 2 February 2025. During daytime, enhanced auroral heating may have modified the background meridional neutral wind circulation, thereby reducing the downward transport of plasma for approximately three hours (11:00–14:00 LT) on 1 February 2025. Also, a contribution from the penetration electric fields associated with substorm activity cannot be ruled out (Wei et al., 2015). The location of Vernadsky Station in a region with a magnetic dip angle of ~57.5° (https://geomag.bgs.ac.uk/data_service/models_compass/wmm_calc.html) also contributes to the sustained influence of neutral winds within the WSA region. Although the maximum efficiency of plasma lifting occurs at dip angles near 45° (Dudeney & Piggott, 1978), at ~60°, this mechanism remains quite effective for maintaining the evening enhancement of N_mF_2. Extended daylight conditions in polar regions during summer additionally maintain photoionisation, further supporting the persistence of the ionosphere.

Despite the pronounced uplift of h_mF_2 (by ~60–70 km) on 1 and 2 February 2025, nighttime N_mF_2 and VTEC values decreased significantly, indicating a weakening of the WSA under geomagnetically disturbed conditions. The observed depletion was likely associated with storm-time changes in neutral composition propagating from high to lower latitudes, as well as enhanced recombination processes during the negative ionospheric storms, as discussed above.

Equatorward neutral winds superimposed on the background thermospheric summer-to-winter circulation produced the observed uplift of the ionosphere. At the same time, there are no clear signatures of vertical plasma transport driven by the penetration electric field of high-latitude origin in the observed h_mF_2 variations. In particular, the absence of h_mF_2 fluctuations associated with electrodynamic forcing (Buonsanto et al., 1999; Richmond & Lu, 2000; Sojka et al., 2002; Goncharenko et al., 2005), despite significant variations in the interplanetary electric field (E_y) (*e.g.,* after 00:00 LT on 1 February), suggests that this mechanism was not the dominant driver of the observed uplift. Another example is the period after 00:00 LT on 2 February, when a pronounced uplift of the ionosphere occurred without corresponding enhancements or rapid changes in the electric field, while N_mF_2 showed a strong depletion.

Thus, the observed ionospheric response to the 1–2 February 2025 storm likely reflects a competition between plasma enhancement due to neutral wind-induced uplift and composition-driven plasma loss. Liu & Yamamoto (2011), in their study of the mid-latitude summer nighttime anomaly, suggested that as the O/N_2 composition disturbance zone, transported by neutral winds, propagates from high to low latitudes with decreasing magnitude, its effect is stronger at the poleward edge of the anomaly. A similar mechanism likely contributed to the observed ionospheric response in the WSA region, where the Vernadsky Station is located close to the poleward edge.

These results demonstrate convincingly that even minor geomagnetic disturbances can significantly affect the WSA.

4 Conclusions

This study investigated the ionospheric WSA response to weak geomagnetic disturbances that occurred on 1–2 February 2025 using ionosondes of the Ukrainian Antarctic Akademik Vernadsky station and the GNSS-based data. The main findings are summarised as follows.

1. A pronounced nighttime depletion was observed in both ionosonde F2-layer peak electron density and GNSS-derived VTEC measurements on 1 and 2 February 2025, indicating the development of the negative phase of the ionospheric storm. N_mF_2 decreased by a factor of ~2 on 1 February and

by a factor of ~5 on 2 February, despite a strong uplift of h_mF_2 by 60—70 km. The VTEC was reduced by ~15—20 TECU and 25 TECU, respectively.

2. The simultaneous decrease in nighttime N_mF_2 and VTEC indicates a weakening of the WSA during a minor geomagnetic storm. This depletion was likely associated with storm-time neutral compositional changes.

3. The observations demonstrate that significant plasma uplift at the WSA region does not guarantee enhanced N_mF_2.

Data availability. The IonogramViewer2 program can be downloaded from the GitHub repository (retrieved on 23 December 2025, from https://github.com/Albom/IonogramViewer2). The ionosonde data are available at the Zenodo data repository (Reznychenko et al., 2026). The NHPC program can be downloaded from the UMass Lowell Space Science Lab website (retrieved on 23 December 2025, from https://ulcar.uml.edu/SoftwareUtilities/NHPC/NHPC430.ZIP). The Vertical TEC data are provided by UPC Global Ionospheric Maps (retrieved on 23 December 2025, from the https://cddis.nasa.gov/archive/gnss/products/ionex/). The K_p index was obtained from the World Data Center for Geomagnetism (https://wdc.kugi.kyoto-u.ac.jp/aedir/), the $F_{10.7}$ solar flux index from https://www.spaceweather.gc.ca/solar_flux_data/daily_flux_values/fluxtable.txt, and the SYM-H index and solar wind parameters to calculate the Akasofu function were taken from the OMNIWeb database (retrieved on 23 December 2025, from https://omniweb.gsfc.nasa.gov/form/omni_min.html).

Author contributions. The idea, data processing, and illustration preparing: M. R., O. B., D. K., and T. Z. Data acquisition and preparation: O. B. and T. Z. Interpretation of the results: O. B., M. R., and D. K. Writing: M. R., D. K., and O. B. Manuscript review and editing: M. R., D. K., O. B., T. Z., K. M., V. B., and V. K. All authors have read and agree to publish the current version of the manuscript.

Acknowledgments. The authors are sincerely grateful to all defenders of Ukraine, volunteers, medics, personnel of emergency and municipal services for the opportunity for Ukrainian scientists to continue their research activities.

Funding. The study was done in the framework of the State Special-Purpose Research Program in Antarctica for 2011—2027. M. R., D. K., and O. B. also acknowledge the EOARD — STCU Partner Project P795 "Diagnostics of natural and manmade ionospheric disturbances over Ukraine". M. R. was also partially supported by Partnership for Excellence in Civil Aviation Space Weather User Services (PECASUS).

Conflict of Interests. The authors declare no conflict of interests.

References

Akasofu, S.-I. (1981). Energy coupling between the solar wind and the magnetosphere. *Space Science Reviews, 28*, 121—190. https://doi.org/10.1007/BF00218810

Bellchambers, W. H., & Piggott, W. R. (1958). Ionospheric measurements made at Halley Bay. *Nature, 182*, 1596—1597. https://doi.org/10.1038/1821596a0

Borries, C., Berdermann, J., Jakowski, N., & Wilken, V. (2015). Ionospheric storms—A challenge for empirical forecast of the total electron content. *Journal of Geophysical Research: Space Physics, 120(4)*, 3175—3186. https://doi.org/10.1002/2015JA020988

Buonsanto, M. J. (1999). Ionospheric storms — A review. *Space Science Reviews, 88*, 563—601. https://doi.org/10.1023/A:1005107532631

Buonsanto, M. J., González, S. A., Lu, G., Reinisch, B. W., & Thayer, J. P. (1999). Coordinated incoherent scatter radar study of the January 1997 storm. *Journal of Geophysical Research: Space Physics, 104*(A11), 24625—24637. https://doi.org/10.1029/1999JA900358

Chakraborty, S., & Seemala, G. K. (2026). Ionospheric responses over the Antarctic region to intense space weather events: Plasma convection vs. auroral precipitation. *Advances in Space Research, 77*(2), 2602—2613. https://doi.org/10.1016/j.asr.2025.10.107

Chen, Y., Liu, L., Le, H., Zhang, H., & Zhang, R. (2022). Responding trends of ionospheric F_2-layer to weaker geomagnetic activities. *Journal of Space Weather and Space Climate, 12*(6). https://doi.org/10.1051/swsc/2022005

Correia, E., Spogli, L., Alfonsi, L., Cesaroni, C., Gulisano, A. M., Thomas, E. G., Ramirez, R. F. H., & Rodel, A. A. (2017). Ionospheric F-region response to the 26 September 2011 geomagnetic storm in the Antarctica American and Australian sectors. *Annales Geophysicae,* *35(5)*, 1113–1129. https://doi.org/10.5194/angeo-35-1113-2017

de Abreu, A. J., Correia, E., de Jesus, R., Venkatesh, K., Macho, E. P., Roberto, M., Fagundes, P. R., & Gende, M. (2023). Statistical analysis on the ionospheric response over South American mid- and near high-latitudes during 70 intense geomagnetic storms occurred in the period of two decades. *Journal of Atmospheric and Solar-Terrestrial Physics, 245*, 106060. https://doi.org/10.1016/j.jastp.2023.106060

Dudeney, J. R., & Piggott, W. R. (1978). Antarctic ionospheric research. In L. J. Lanzerotti & C. G. Park (Eds.), *Upper atmospheric research in Antarctica* (Antarctic Research Series, Vol. 29, pp. 200–235). American Geophysical Union.

Emmert, J. T. (2015). Thermospheric mass density: A review. *Advances in Space Research, 56*(5), 773–824. https://doi.org/10.1016/j.asr.2015.05.038

Fuller-Rowell, T. J. (2011). Storm-time response of the thermosphere-ionosphere system. In M. A. Abdu & D. Pancheva (Eds.), *Aeronomy of the Earth's atmosphere and ionosphere* (IAGA Special Sopron Book Series, Vol. 2, pp. 419–435). Springer. https://doi.org/10.1007/978-94-007-0326-1_32

Fuller-Rowell, T. J., Codrescu, M. V., Moffett, R. J., & Quegan, S. (1994). Response of the thermosphere and ionosphere to geomagnetic storms. *Journal of Geophysical Research: Space Physics, 99*(A3), 3893–3914. https://doi.org/10.1029/93JA02015

Fuller-Rowell, T. J., Codrescu, M. V., Rishbeth, H., Moffett, R. J., & Quegan, S. (1996). On the seasonal response of the thermosphere and ionosphere to geomagnetic storms. *Journal of Geophysical Research: Space Physics, 101*(A2), 2343–2353. https://doi.org/10.1029/95JA01614

Gao, Q., Liu, L.-B., Zhao, B. Q., Wan, W.-X., Zhang, M.-L., & Ning, B.-Q. (2008). Statistical study of the storm effects in middle and low latitude ionosphere in the East-Asian sector. *Chinese Journal of Geophysics, 51*(3), 435–443. https://doi.org/10.1002/cjg2.1234

Goncharenko, L. P., Salah, J. E., van Eyken, A., Howells, V., Thayer, J. P., Taran, V. I., Shpynev, B., Zhou, Q., & Chau, J. (2005). Observations of the April 2002 geomagnetic storm by the global network of incoherent scatter radars. *Annales Geophysicae, 23*(1), 163–181. https://doi.org/10.5194/angeo-23-163-2005

Gonzalez, W. D., Joselyn, J. A., Kamide, Y., Kroehl, H. W., Rostoker, G., Tsurutani, B. T., & Vasyliunas, V. M. (1994). What is a geomagnetic storm? *Journal of Geophysical Research: Space Physics, 99*(A4), 5771–5792. https://doi.org/10.1029/93JA02867

Hernández-Pajares, M., Juan, J. M., Sanz, J., Orus, R., García-Rigo, A., Feltens, J., Komjathy, A., Schaer, S. C., & Krankowski, A. (2009). The IGS VTEC maps: A reliable source of ionospheric information since 1998. *Journal of Geodesy, 83*(3–4), 263–275. https://doi.org/10.1007/s00190-008-0266-1

Hernández-Pajares, M., Juan, J. M., Sanz, J., Aragón-Angel, A., García-Rigo, A., Salazar, D., & Escudero, M. (2011). The ionosphere: Effects, GPS modeling and the benefits for space geodetic techniques. *Journal of Geodesy, 85*(12), 887–907. https://doi.org/10.1007/s00190-011-0508-5

Hernández-Pajares, M., Roma-Dollase, D., Krankowski, A., García-Rigo, A., & Orús-Pérez, R. (2017). Methodology and consistency of slant and vertical assessments for ionospheric electron content models. *Journal of Geodesy, 91*, 1405–1414. https://doi.org/10.1007/s00190-017-1032-z

Horvath, I., & Essex, E. A. (2003). The Weddell Sea anomaly observed with the TOPEX satellite data. *Journal of Atmospheric and Solar-Terrestrial Physics, 65*(6), 693–706. https://doi.org/10.1016/S1364-6826(03)00083-X

Huang, X., & Reinisch, B. W. (1996). Vertical electron density profiles from the Digisonde network. *Advances in Space Research, 18(6)*, 121–129. https://doi.org/10.1016/0273-1177(95)00912-4

Koloskov, O., Kashcheyev, A., Bogomaz, O., Sopin, A., Gavrylyuk, B., & Zalizovski, A. (2023). Performance analysis of a portable low-cost SDR-based ionosonde. *Atmosphere, 14(1)*, 159. https://doi.org/10.3390/atmos14010159

Liu, H., & Yamamoto, M. (2011). Weakening of the mid-latitude summer nighttime anomaly during geomagnetic storms. *Earth, Planets and Space, 63*, 371–375. https://doi.org/10.5047/eps.2010.11.012

Mansilla, G. A. (2017). Response of the Antarctic ionosphere to some intense geomagnetic storms. *The Open Atmospheric Science Journal, 11*, 16–28, https://doi.org/10.2174/1874282301711010016. https://benthamopen.com/contents/pdf/TOASCJ/TOASCJ-11-16.pdf

Melendi, Y. D., Bravo, M., Molina, M. G., Paz, M., Urra, B., De Pasquale, L., Scipión, D. E., Namour, J., Duran, T., & Zalizovski, A. (2025). Global and regional ionospheric response to a moderate storm in South America and Antarctica using a multi-instrumental approach. *Earth and Space Science, 12(8)*, e2025EA004281. https://doi.org/10.1029/2025EA004281

Mendillo, M. (2006). Storms in the ionosphere: Patterns and processes for total electron content. *Reviews of Geophysics, 44*(4), RG4001. https://doi.org/10.1029/2005RG000193

Perreault, P., & Akasofu, S. I. (1978). A study of geomagnetic storms. *Geophysical Journal International, 54(3)*, 547–573. https://doi.org/10.1111/j.1365-246X.1978.tb05494.x

Piggott, W. R., & Rawer, K. (1972). *URSI handbook of ionogram interpretation and reduction*. World Data Center A for Solar-Terrestrial Physics, Report UAG-23A.

Prölss, G. W. (1997). Magnetic Storm Associated Perturbations of the Upper Atmosphere. In B. T. Tsurutani, W. D. Gonzalez, Y. Kamide & J. K. Arballo (Eds.), *Magnetic Storms* (pp. 227–241). https://doi.org/10.1029/GM098p0227

Prölss, G. W. (2004). *Physics of the Earth's space environment: An introduction*. Springer. https://doi.org/10.1007/978-3-642-97123-5

Qian, L., Solomon, S. C., & Kane, T. J. (2009). Seasonal variation of thermospheric density and composition. *Journal of Geophysical Research: Space Physics, 114(A1)*, A01312. https://doi.org/10.1029/2008JA013643

Reznychenko, M., Bogomaz, O., Kotov, D., Zhivolup, T., Burmaka, V., & Kolodyazhnyi, V. (2026). *Raw ionogram data from Akademik Vernadsky station* (*Jan 30 – Feb 5, 2025*) [Data set]. Zenodo. https://doi.org/10.5281/zenodo.19480381

Richmond, A. D., & Lu, G. (2000). Upper-atmospheric effects of magnetic storms: A brief tutorial. *Journal of Atmospheric and Solar-Terrestrial Physics, 62*(12), 1115–1127. https://doi.org/10.1016/S1364-6826(00)00094-8

Sojka, J. J., David, M., & Schunk, R. W. (2002). A mid-latitude space weather hazard driven directly by the magnetosphere. *Journal of Atmospheric and Solar-Terrestrial Physics, 64*(5–6), 687–695. https://doi.org/10.1016/S1364-6826(02)00030-5

Wei, Y., Zhao, B., Guozhu, L., & Wan, W. (2015). Electric field penetration into Earth's ionosphere: A brief review for 2000–2013. *Scientific Bulletin*, *60*(8), 748–761. https://doi.org/10.1007/s11434-015-0749-4

Received: 3 March 2026
Accepted: 28 May 2026
Published: 3 July 2026

Реакція іоносфери на слабку геомагнітну бурю 1–2 лютого 2025 року у регіоні аномалії моря Ведделла: спостереження на Українській антарктичній станції «Академік Вернадський»

Марина Резниченко[1, 2, *], Олександр Богомаз[1, 3], Дмитро Котов[1], Тарас Живолуп[1], Катерина Мартинова[1], Віктор Бурмака[1], Вячеслав Колодяжний[1]

[1] Інститут іоносфери, Національний технічний університет «Харківський політехнічний інститут», м. Харків, 61002, Україна

[2] Центр космічних досліджень Польської академії наук, м. Варшава, 00-716, Польща

[3] Радіоастрономічний інститут Національної академії наук України, м. Харків, 61002, Україна

*** Автор для кореспонденції:** mrezn.cbk@gmail.com

Реферат. Досліджено реакцію іоносфери на слабку геомагнітну бурю 1–2 лютого 2025 року в регіоні аномалії моря Ведделла. Проаналізовано поведінку ключових параметрів іоносфери (N_mF_2 та h_mF_2) за даними іонозондових спостережень на Українській антарктичній станції «Академік Вернадський», а також повного електронного вмісту у вертикальному стовпі, отриманого за допомогою вимірювань глобальної навігаційної супутникової системи. Значне зменшення концентрації електронів шару F2 іоносфери (N_mF_2) та повного електронного вмісту спостерігалося в нічні години 1-го та 2-го лютого 2025 року. Це свідчить про розвиток негативної фази іоносферної бурі та послаблення аномалії моря Ведделла під час слабких геомагнітних збурень. N_mF_2 зменшилася приблизно в 2 рази 1 лютого та приблизно в 5 разів 2 лютого, тоді як повний електронний вміст зменшився на ~15–20 TECU та ~25 TECU, відповідно. Негативна фаза поширювалася значно далі в напрямку екватора 1 лютого, тоді як 2 лютого вона залишалася обмеженою високими та середніми широтами. Примітно, що настільки суттєве зменшення N_mF_2 відбулося попри значне підняття висоти максимуму шару F2 іоносфери (h_mF_2) на ~60–70 км. Чітких ознак вертикального переносу плазми, зумовленого проникненням електричного поля, у варіаціях h_mF_2 не виявлено. Ймовірною причиною такого зменшення концентрації іоносферної плазми є зміни нейтрального складу під час бурі, пов'язані з апвелінгом, зменшенням відношення O/N_2 та перенесенням зони збуреного нейтрального складу термосферними вітрами від високих до нижчих широт. Отримані результати демонструють, що навіть слабкі геомагнітні бурі можуть суттєво модифікувати систему іоносфера–термосфера над Антарктикою та значно впливати на аномалію моря Ведделла.

Ключові слова: іонозонд, іоносфера, іоносферна буря, концентрація електронів, негативна фаза, шар F2